Regulating the β′→β Polymorphic Transition in Food Fats

D. Rousseau[a,*], S.M. Hodge[a], M.T. Nickerson[b], and A.T. Paulson[b]

[a]School of Nutrition, Ryerson University, Toronto, Ontario, Canada M5B 2K3, and [b]Department of Food Science and Technology, Dalhousie University, Halifax, Nova Scotia, Canada B3J 2X4

ABSTRACT: Hydrogenated cottonseed oil (HCSO) is commonly used as a β′-stable fat in margarines and shortenings. In the present study, the crystallization behavior of HCSO is altered *via* dilution, agitation, tempering regime, and the addition of an emulsifier [polyglycerol polyricinoleate (PgPr)]. Key properties assessed include crystal morphology (with polarized light microscopy), polymorphic behavior (with X-ray diffraction), and crystallization kinetics (with DSC). It is demonstrated that on considerable dilution with canola oil (4% w/w), HCSO can be crystallized in the β′ or β polymorph with associated changes in crystal morphology, depending on tempering regime. Crystallization from the melt to 25°C results in the β′-form, as there is insufficient supercooling to form the β polymorph but enough to form the metastable β′. With cooling from the melt to 5°C, there is adequate supercooling for the β polymorph to form, with the presence of the canola oil facilitating the transformation toward this stable phase. Static vs. crystallization under agitation does not lead to visible changes in either polymorphic behavior or crystal morphology. However, there is extensive secondary nucleation and growth as a result of crystals breaking off accreting agglomerates. The presence of PgPr, added as a crystal modifier, does not affect the final crystal polymorph or morphology, except under one set of conditions—crystallization from the melt to 5°C with agitation, whereby it considerably alters crystallization behavior.

Paper no. J10820 in *JAOCS 82*, 7–12 (January 2005).

KEY WORDS: Agitation, cottonseed oil, crystallization, dilution, PgPr, polymorphism.

Composition, tempering regime, the presence of other lipids or additives, and mechanical treatment (e.g., shear, agitation) influence how a lipid solidifies from the melt. In the food industry, these parameters are all used to direct polymorphic behavior and morphological development in fats. For example, in margarine production, maintaining β′-crystallinity is imperative to preserve smooth texture and acceptable spreadability. This is achieved by using naturally β′-stable fats, by blending β-stable fats with non-β-tending fats, and/or by using emulsifiers (typically 0.1–0.5% w/w), such as MAG or sorbitan tristearate, that hinder the β′→β transition. In chocolate manufacture, careful tempering is used to promote the crystallization of the metastable β-V form of cocoa butter, responsible for much of chocolate's organoleptic and shelf life properties.

*To whom correspondence should be addressed at School of Nutrition, Ryerson University, 350 Victoria St., Toronto, Ontario, Canada M5B 2K3. E-mail: rousseau@ryerson.ca

In fats, the kinetics of the system will favor the formation of a metastable form (e.g., usually, but not always, the α-form), whereas the thermodynamics will promote formation of the more stable form (sometimes β′ and usually β). Nucleation and growth of the metastable form will normally predominate, in accordance with Ostwald's law of stages. In this regard, the majority of our growing knowledge on polymorphic transformations in fats is based on model systems consisting of either single TAG or simple mixtures thereof. By comparison, we have yet to answer many of the vagaries associated with the crystallization of natural fats.

As part of a long-term endeavor focusing on the kinetic stabilization of emulsions with low concentrations of continuous-phase crystals, the present study investigates the polymorphism and morphology of hydrogenated cottonseed oil (HCSO), which is normally used as a β′-tending fat in margarine and shortening production. We show that its final (stable) polymorphic form and morphology can be manipulated through a multipronged approach involving dilution, tempering regime, presence of polyglycerol polyricinoleate (PgPr), and under different crystallization conditions (static vs. dynamic crystallization).

MATERIALS AND METHODS

Additive-free fully refined, bleached, and deodorized flaked fully hydrogenated cottonseed oil (HCSO) and refined, bleached, and deodorized canola oil (CO) were gifts from CanAmera Foods (Toronto, Canada) and were used without further purification. PgPr, a lipophilic emulsifier (hydrophilic-lipophilic balance < 5), is used in margarine to stabilize β′ fats and in chocolate to improve its viscosity characteristics. It was obtained from Nealanders International (Mississauga, Ontario, Canada). Solutions of 4% (w/w) HCSO (50-g samples in a 250-mL beaker) in CO were crystallized to either 5 or 25°C from the melt. All samples, with or without agitation (240 rpm, using a blade-type impeller) and with or without the presence of PgPr [0.125% (w/w)] were crystallized under very similar cooling conditions. Numerous samples were crystallized to confirm homogeneity in the temperature profile. Examples of the cooling curves for dynamically and statically cooled samples are shown in Figure 1. In both examples, temperature probes were near the center of the samples.

To characterize the TAG composition of the base fats, capillary GC (PE XL; PerkinElmer, Markham, Ontario, Canada) was performed, following AOCS Method Ce 5-86 (1). The capillary column was a 4-m Supelco Petrocol column (i.d. 0.53 mm)

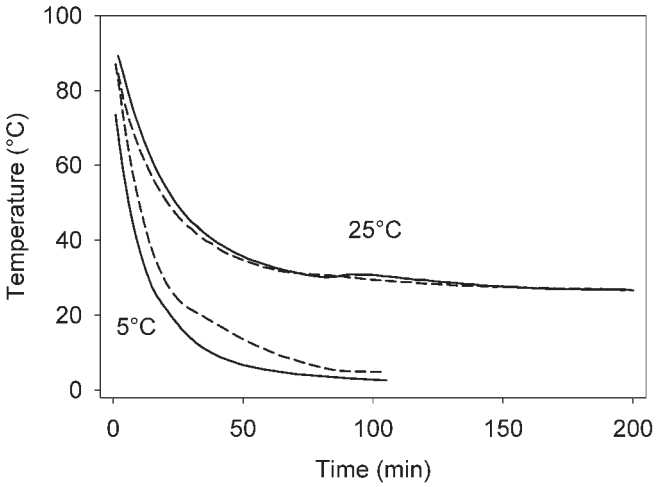

FIG. 1. Cooling curves for 4% (w/w) hydrogenated cottonseed oil (HCSO) in canola oil (CO) from the melt to 25°C (upper curves) or 5°C (lower curves). Solid line: static cooling; dotted line: cooling with agitation. See text for experimental conditions.

(Belleville, Ontario, Canada). Sample on-column injection (1 μL) at 70°C was followed by a temperature ramp to 170°C at 20°C/min; a ramp from 170 to 350°C at 15°C/min was then used. All TAG species eluted by 350°C. The injector temperature was maintained at 5°C above oven temperature. The carrier gas was helium at 3.7 mL/min, and detector gases were hydrogen at 45 mL/min and air at 450 mL/min. Species with carbon numbers below 46 amounted to 1.2% in HCSO and 1.1% in CO. AOCS Official Method Ca 5a-40 was used for determination of total FFA (1). FFA content, expressed as percent oleic acid (w/w), was 0.017 ± 0.02% in CO and 0.018 ± 0.003% in HCSO.

Solid fat content (SFC) of the HCSO as a function of temperature was evaluated using a Bruker Minispec Mq pulsed NMR (pNMR) unit (Bruker Canada, Milton, Ontario, Canada), following AOCS Official Method Cd 16b-93 (1).

Calorimetric data were collected with a TA Instruments Q100 differential scanning calorimeter (TA Instruments-Waters LCC, New Castle, DE) equipped with a refrigerated cooling system. The instrument was calibrated with gallium (Sigma-Aldrich Co., St. Louis, MO; 99.999% purity) and flushed with nitrogen (15 mL/min). Thermal analysis was performed on three different samples: 100% HCSO, 4% (w/w) HCSO in CO, and 4% (w/w) HCSO in CO with 0.125% (w/w) PgPr. Samples (~4–5 mg) were placed into hermetically sealed aluminum pans, and an empty pan was used as a reference. Thermal cycles mimicking the cooling regimes shown in Figure 1 were performed: (i) Melt to 25°C: Samples, heated to 93°C and held for 5 min, were cooled to 35°C at 1.25°C/min, then to 25°C at 0.07°C/min, where they were held isothermally for 15 min. (ii) Melt to 5°C: Samples, heated to 93°C and held for 5 min, were cooled to 25°C at 2.8°C/min, then to 5°C at 0.35°C/min, where they were held isothermally for 60 min. Data were analyzed using the instrument software. All samples for each thermal cycle were measured in duplicate.

Polarized light microscopy (PLM) was used to examine the morphology of the diluted HCSO under different crystallization conditions. Samples were placed on viewing slides (Fisher, St. Louis, MO), on which a cover slip (Fisher) was gently placed. A 20× plan-apochromat objective was used for visual examination using a Zeiss LSM510 confocal laser scanning microscope (Zeiss, Toronto, Canada). Sample temperature was maintained with an Instec STC-200 temperature-controlled stage. Images were captured with a Q-Imaging CCD camera and analyzed using Northern Eclipse software (version 6.0; Empix Imaging, Burlington, Ontario, Canada). Many samples were examined, and each photomicrograph represents a typical field, taken from near the middle of the sample beakers.

A Rigaku Geigerflex (Danvers, MA) X-ray diffraction (XRD) unit (λ = 1.79 Å) was used to determine the powder diffractograms of the HCSO samples at 25°C, subjected to the cooling regimes shown in Figure 1. Scans from 1.5 to 40° 2θ were performed. Sample preparation was meticulously controlled to ensure reproducibility in XRD spectra. All analyses were performed in triplicate.

RESULTS AND DISCUSSION

Characteristics of base materials. The key TAG groups in CO (Fig. 2) were C_{52} (11.6%), C_{54} (78.5%), and C_{56} (6.2%). In HCSO, the key TAG were C_{50} (16.4%), C_{52} (42.5%), and C_{54} (34.8%). Given that the cottonseed oil was fully hydrogenated [iodine value (IV) = 1], the TAG species in the HCSO were 2-stearyldipalmitin (PSP) (C_{50}), 1-palmityldistearin (PSS) (C_{52}), and tristearin (SSS) (C_{54}) (2,3). In canola oil, the primary TAG were fully unsaturated (oleic + linoleic).

The physical properties of the 100% HCSO examined in this work included SFC, crystallization behavior, and polymorphic form. The SFC vs. temperature evolution in HCSO indicated that significant melting occurred between 55 and 65°C (Fig. 3). The polymorphic behavior of the flake HCSO comprised a very strong long-spacing at 44.6 Å, a medium reflection at 14.98 Å, and a very weak reflection at 9.01 Å. Strong short-spacings (Fig. 4) existed at 3.79 Å, 4.21 Å, and

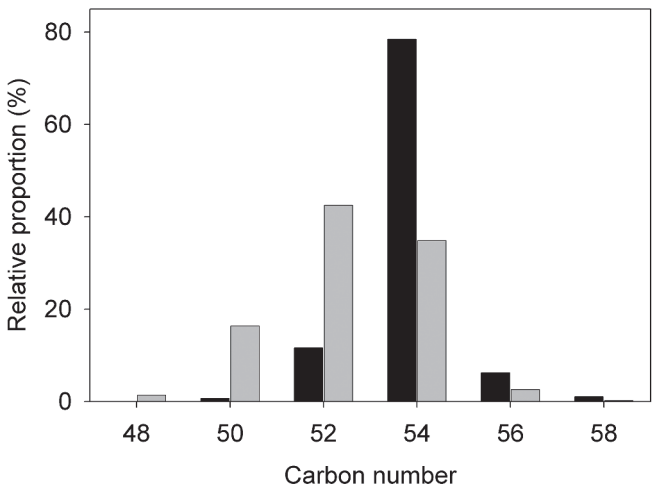

FIG. 2. Relative TAG proportions in HCSO and CO, based on carbon numbers. Grey bars, HCSO; solid bars, CO. For abbreviations see Figure 1

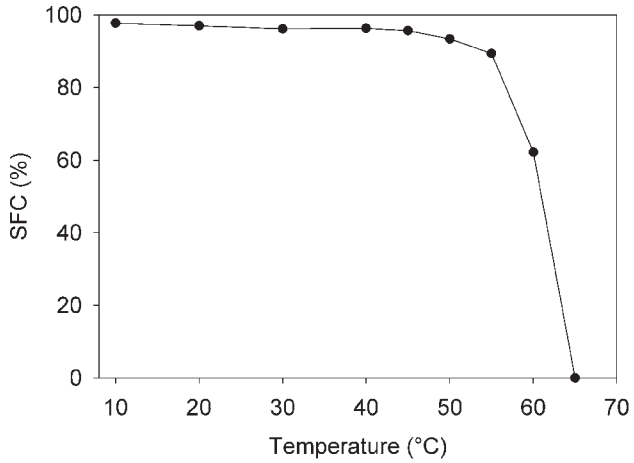

FIG. 3. Solid fat content (SFC) vs. temperature evolution in HCSO. For other abbreviation see Figure 1.

a doublet at 4.33/4.34 Å. These results indicated that the flake HCSO existed as a double layer in the β′-form (β′-2) (3). Riiner (4) noted similar short-spacings in partially hydrogenated (IV = 67.8) cottonseed oil, whereas fully hydrogenated cottonseed oil had a strong spacing at 3.8 Å and a diffuse, yet strong spacing at 4.2 Å. Last, the crystallization thermogram of 100% HCSO, obtained *via* DSC, showed a single peak at ~48°C with a corresponding enthalpy of ~99 J/g (Fig. 5). A shoulder was visible, likely indicative of a second fraction. As mentioned above, however, no β-crystallinity was detected in the 100% HCSO under either cooling regime. Thus, this fraction was also in the β′-form.

Diluted HCSO crystallization behavior. (i) Cooling to 25°C. Under these conditions, HCSO polymorphism was largely unaffected by either agitation or the presence of PgPr, with all samples existing in the β′-2 form (Table 1). In double-layer structures, the odd-order long-spacings are much stronger than the even-order long-spacings (5,6), and such behavior has often been observed (7,8). Lutton *et al.* (7) showed that the first-order reflection of PSP occurred at 42.8 Å,

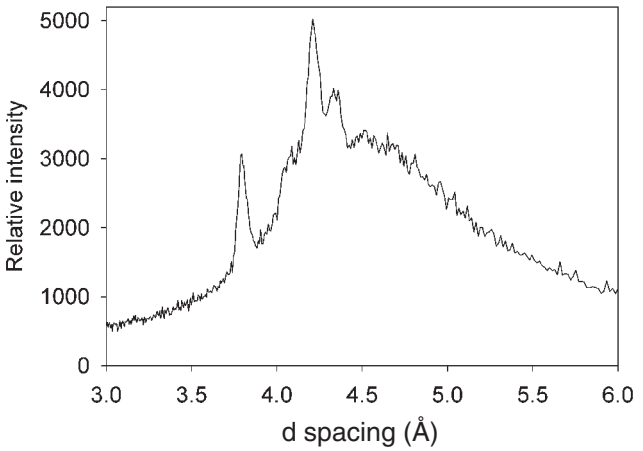

FIG. 4. Short-spacings of flake HCSO as evaluated by powder X-ray diffraction. For abbreviation see Figure 1.

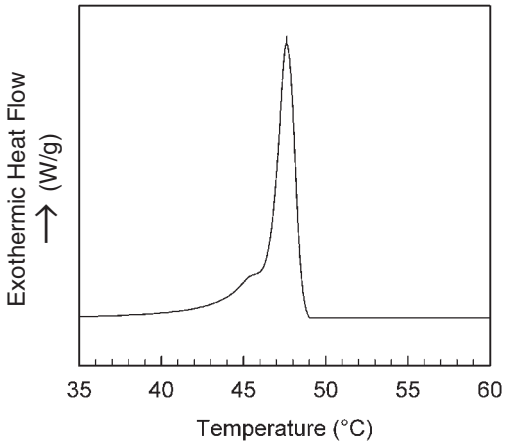

FIG. 5. DSC thermogram of 100% HCSO. For abbreviation see Figure 1.

whereas the first-order reflection of SSS and PSS in the β′-form occurred at 46.8 and 45.1 Å. Thus, the β′-spectrum of diluted HCSO was dominated by PSP, not SSS and PSS.

PLM (Fig. 6) showed that samples crystallized to 25°C consisted of agglomerated platelets, with slight differences based on crystallization environment. Statically crystallized HCSO structures averaged ~50 μm in diameter and ranged from 15 to 150 μm in diameter (Fig. 6A). HCSO crystallized under agitation consisted of structures averaging diameters of ~100 μm with smoothed edges compared to the statically crystallized HCSO (Fig. 6B). Van Putte and Bakker (9) noted a similar phenomenon with palm oil crystallization, whereby spherulites grown under agitation were smoother than those crystallized statically. In our samples, there was a great size distribution among structures in samples crystallized under agitation, likely due to secondary nucleation resulting from crystals breaking off from agglomerates and promoting further nucleation (10). It appears that the secondary nuclei/crystals in the form of platelets between large groups sintered, forming solid bridges. Statically crystallized HCSO in the presence of PgPr (Fig. 6C) resulted in agglomerates similar to Figure 6A with well-defined edges, averaging ~40 μm in diameter. Finally, with the combination of agitation and PgPr, agglomerates were large, averaging ~100 μm in diameter. Crystals not associated with agglomerates were visible, the result of agitation, as noted above.

(ii) Cooling to 5°C. Diluted HCSO cooled to 5°C crystallized primarily in the β-form. In all samples, greater supercooling led to an increased number of crystals that were smaller than at 25°C.

TABLE 1
Long- and Short-Spacings[a] for All Samples Crystallized from the Melt to 25°C

Long-spacings	Short-spacings
d(001) = 43.2 VS	3.78 S
d(003) = 14.93 M	4.06 M
d(004) = 11.28 VW	4.19 VS
d(005) = 8.97 W	4.33 M

[a]V, very; S, strong; M, medium; W, weak.

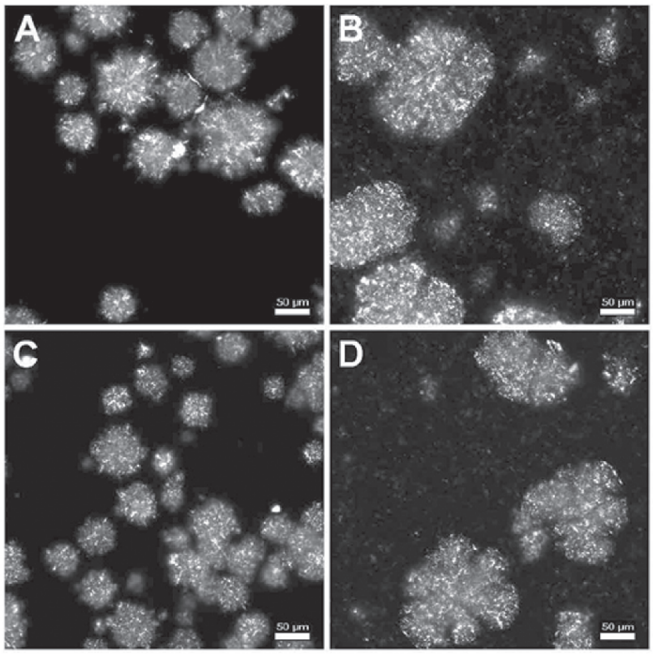

FIG. 6. Polarized light microscopy (PLM) images of 4% (w/w) HCSO in CO crystallized at 25°C. (A) Static crystallization; (B) crystallization with agitation; (C) static crystallization with polyglycerol polyricinoleate (PgPr); (D) crystallization with agitation and PgPr. For other abbreviations see Figure 1.

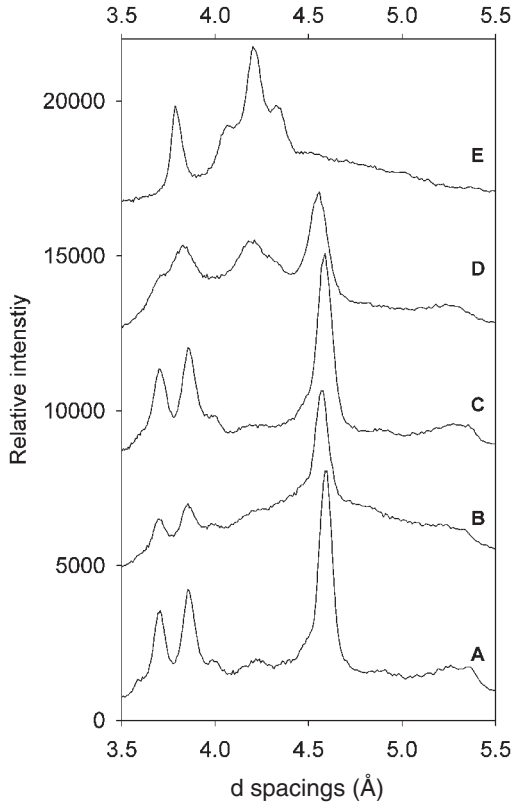

FIG. 7. Short-spacings of 4% (w/w) HCSO crystallized to 5°C. (A) Static crystallization; (B) crystallization with agitation; (C) static crystallization with PgPr; (D) crystallization with agitation and PgPr. (E) putative results from 25°C crystallization. For abbreviations see Figures 1 and 6.

Long-spacings for statically crystallized samples with and without agitation saw their d(001) reflections increase by >1 Å (Table 2), compared with crystallization at 25°C. Higher-order reflections were not as well defined in HCSO crystallized under agitation. Static crystallization in the presence of PgPr resulted in a 1-Å decrease in the d(001) reflection. The combined effects of agitation and PgPr produced substantial changes in unit cell length, with a ~3-Å decrease in lamellar size compared with the statically crystallized PgPr-free diluted HCSO. Lutton *et al.* (7) showed that the first-order reflection of SSS (β-form) occurred at 45.15 Å, whereas the first-order reflection of PSS occurred at 44.7 Å (also β-form). Thus, the β-spectrum of diluted HCSO was dominated by these two TAG species, and not PSP.

The short-spacings yielded substantial information on HCSO's crystallization behavior (Fig. 7). The short-spacings of the HCSO statically crystallized with and without PgPr were very close (spectra A and C), demonstrating strong β-crystal spacings, at 3.69, 3.86, and 4.59 Å. Quite interesting is the presence of a peak in the 5.25–5.35 Å region. Lutton *et al.* (7) showed that the β-form of SSS is in part characterized by a medium-spacing at 5.24 Å, whereas the β-form of PSS shows a reflection at 5.34 Å. Thus, the short-spacings observed appear to be a combination of SSS and PSS. The spectrum of HCSO crystallized with agitation (spectrum B) was also similar, although the reflections were not as strong, possibly indicating a "destructuring" of the crystal lamellae. Last, the combined effect of agitation and PgPr produced significant changes in short-spacings, with the disappearance of the reflections at 3.69 Å, and the shifting of peaks at 3.86 and 4.59 Å to 3.82 and 4.55 Å, respectively (spectrum D). Furthermore, there was a large "hump" in the 4.02–4.40 Å region. These observations point to this sample simultaneously existing in the α, β′, and β forms and possibly showing substantially altered crystallization kinetics. For comparison, putative short-spacings of HCSO crystallized at 25°C are shown (spectrum E).

PLM of samples crystallized to 5°C (Fig. 8) showed that the morphology of the crystals was spherulitic for all samples, although they were much smaller than the agglomerates in the 25°C regime. All treatments consisted of spherulites in the 15–20 µm range. The morphology differed slightly for HCSO crystallized under agitation in the presence of PgPr, appearing denser than with other treatments.

TABLE 2
Long–Spacings[a] for Samples Crystallized from the Melt to 5°C

	Static crystallization	Crystallization with agitation
No PgPr	d(001) = 44.60 VS	d(001) = 44.60 VS
	d(003) = 14.77 M	d(003) = 14.77 M
	d(005) = 8.86 W	d(005) = 8.71 VW
	d(006) = 7.34 VW	
PgPr	d(001) = 43.65 VS	d(001) = 41.87 VS
	d(003) = 14.77 M	d(003) = 14.56 M
	d(004) = 10.81 VW	d(005) = 8.82 W
	d(005) = 8.78 W	d(006) = 7.27 VW
	d(006) = 7.29 W	

[a]PgPr, polyglycerol polyricinoleate; for other abbreviations see Table 1. See text for experimental conditions.

Mechanistic considerations. The following section describes the concerted roles on HCSO crystallization of dilution, temperature regime, agitation, and addition of PgPr.

In many processed foods, a fat will often be mixed, and hence diluted, with an oil to obtain desired physical, nutritional, and rheological properties. As stated by many (11–13), many naturally occurring fats are driven to their most stable polymorphic form on dilution (e.g., hydrogenated soybean oil, butterfat), when allowed to do so. With diluted HCSO, crystallization at 25°C should have allowed the HCSO TAG greater freedom to adopt a more thermodynamically favorable conformation, this being the β-form. As already shown (Fig. 4), 100% HCSO is β′-stable. It is only on dilution that it can "tuned" to a β′ or β-form. How does dilution influence the β′→β transition? Do vegetable oil TAG introduce themselves into the crystal lattice? This is unlikely. Given the large differences in m.p. between canola oil and HCSO, these do not interact (i.e., they will not form a solid solution). In a study on the mixing behavior of tripalmitin (PPP) and SSS in triolein (OOO), Norton *et al*. (14) conclusively showed that there was no interdigitation or incorporation of OOO into the lattice of PPP on cooling. This may in part be explained by the oleic hydrocarbon chains in OOO which, given their *cis*-bond, are kinked and consequently do not fit into the lattice of crystallizing TAG (15). As a result, taking into consideration that a β′→β polymorphic transition will depend on how well the TAG can rearrange themselves into the more stable orientation, dilution should allow TAG in dilute HCSO to rotate freely and adopt a lower energy state. In 100% HCSO (which was fully solid at both 25 and 5°C) (Fig. 3), irregularities due to different chain lengths and chain penetration in adjacent layers create an energy barrier that is larger than in pure TAG (16). As HCSO contains both PSP (β′-stable) and SSS/PSS (β-stable), there may be segregation for the different TAG, which may explain the broad first-order long-spacings (17). These results also suggest that there is little rotational freedom in the crystal lattices in the 100% HCSO and that the PSP appears to prevent the β′→β transition. In the diluted HCSO, however, as there is only a maximum of 4% SFC, the PSP cannot dissuade the β′→β transition because the SSS and PSS can likely phase-separate from the PSP and be driven to their most thermodynamically favorable form, the β-polymorph.

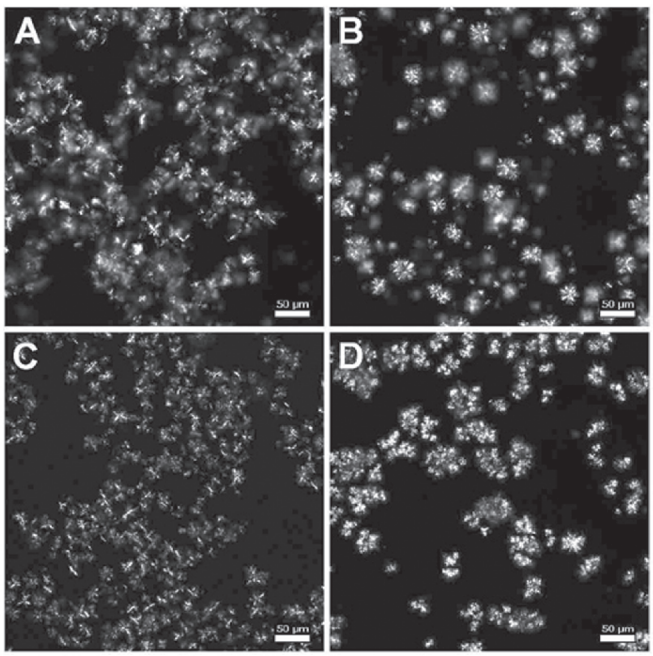

FIG. 8. PLM images of 4% (w/w) HCSO in CO crystallized at 5°C. (A) Static crystallization; (B) crystallization with agitation; (C) static crystallization with PgPr; (D) crystallization with agitation and PgPr. For abbreviations see Figures 1 and 6.

In conjunction with the dilution effect, the cooling regime played a key role in determining the polymorphic pathway. The cooling rates to 5 and 25°C were by no means rapid. Thus, it would be incorrect to speak of quench-cooling in either scenario. With cooling to 25°C, there was obviously lower supersaturation in the system. In such a situation, incorporation of new TAG into the crystal lattice should have taken place only if they were in the right configuration, as they had more time to orient themselves and pack correctly than under high supersaturation conditions (*viz*., cooling to 5°C). This equilibration process should have resulted in the formation of more stable crystals owing to the repeated resolubilization and recrystallization of the molecules. At a higher rate of supercooling, molecules typically attach to crystals more quickly, leading to more imperfect crystals (e.g., more steps, more dislocations, etc.).

Undiluted HCSO was conclusively shown to be β′-stable, irrespective of the cooling regime (Fig. 4). With the diluted HCSO, cooling to 25°C should have resulted in a more stable polymorph, whereas cooling to 5°C initially would yield a metastable form of HCSO that would subsequently transform on annealing to the next most stable state. However, in conjunction with the dilution effect, greater supercooling promoted a β-stable HCSO whereas lower supercooling resulted in a β′-stable crystal structure (it remained stable for at least 12 wk). Increasing supersaturation by lowering the temperature thermodynamically favored the β-form.

DSC of the crystallization kinetics of the diluted HCSO to 5 or 25°C shows enthalpies of 4.3–5.2 J/g for all crystallization events. Crystallization kinetics of the diluted HCSO reveal that the β′→β transition is not visible at 25°C (Fig. 9A). When cooling to 5°C (Fig. 9B), DSC results show two neighboring thermal events. There are two possible explanations for this. Either a solid-state β′→β transformation by at least one, and likely more, species is taking place or, given the slow cooling rate (0.35°C/min), different TAG are distinguishable. Another notable point is that, given that no β′ is visible in the XRD pattern, the PSP must convert to the β-form. While it is normally β′-stable, Lutton (18) stated that a β-polymorph of PSP may be obtained by low-temperature crystallization from a solvent, albeit with difficulty.

An α-form was not visible in either cooling regime. Riiner (4) noted a similar phenomenon with numerous hydrogenated fats. In a study on intersolubility of PSP, 2-oleyldipalmitin, and SSS, Gibon *et al.* (8) found that the β′-form crystallized *via* the α-form was less stable than when crystallized from the melt and

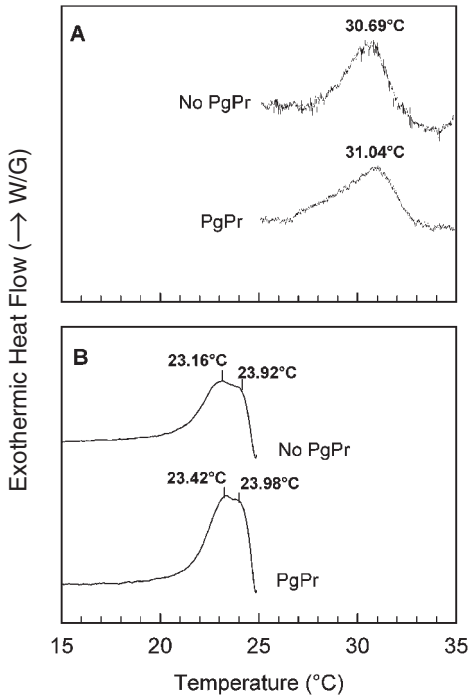

FIG. 9. DSC thermograms of 4% (w/w) HCSO in CO, with and without addition of PgPr. (A) Melt to 25°C; (B) melt to 5°C. Cooling regimes are described in the Materials and Methods section. For abbreviations see Figures 1 and 6.

attributed this to crystal perfection. *Ipso facto*, cooling to 25°C provided insufficient supersaturation to induce a β′→β transformation and instead led to a more highly ordered β′. With cooling to 5°C, a more poorly formed β′ transformed very quickly to β. Similar results have been found in polymers where quenched and annealed systems reach their equilibrium density much more quickly than those isothermally crystallized. Dafler (19) also observed such phenomena with fully saturated TAG and fats, noting that rapidly cooled SSS could reach the β-form more quickly than its isothermally crystallized counterpart. He suggested that in smaller crystalline domains, a faster transition to the stable polymorph was achievable. Last, grain boundaries imparted a "working space" for the relief of lattice strain during the polymorphic transformation.

The role of PgPr and agitation on HCSO crystallization behavior was generally minor. With crystallization to 25°C, neither PgPr nor agitation influenced crystallographic dimensions of the HCSO crystals, although agitation did lead to larger agglomerates, likely owing to enhanced mass transfer that permitted greater platelet accretion. PgPr was not likely included in the lattice, or if it was, did not influence either the short- or long-spacings. Liquid emulsifiers (e.g., PgPr) are not as likely as solid surfactants (e.g., saturated MAG) to fit into crystal lattices (3,20). Cooling to 5°C yielded similar results, except under one set of conditions—PgPr combined with agitation. These results suggested that PgPr retarded the α→β′→β transformation, but only with agitation. Static crystallization in the presence of PgPr indicated no differences in short-spacings or long-spacings. It is possible that under agitation, PgPr was incorporated within "inclusions" in the forming crystals. These inclusions would only be present at the nanoscopic level as PLM did not reveal appreciable differences in microstructure. This event was not visible at 25°C, as the driving force was too low to induce this phenomenon.

REFERENCES

1. *Official Methods and Recommended Practices of the American Oil Chemists' Society*, 5th edn., AOCS Press, Champaign, 1997.
2. Chang, M.-K., G. Abraham, and V.T. John, Production of Cocoa Butter-like Fat from Interesterification of Vegetable Oils, *J. Am. Oil Chem. Soc. 67*:832–834 (1990).
3. Timms, R.E., Phase Behavior of Fats and Their Mixtures, *Prog. Lipid Res. 23*:1–38 (1984).
4. Riiner, U., Investigation of the Polymorphism of Fats and Oils by Temperature Programmed X-Ray Diffraction, *Lebens.-Wiss. Technol. 3*:101–106 (1970).
5. Sato, K., T. Arishima, Z.H. Wang, K. Ojima, N. Sagi, and H. Mori, Polymorphism of POP and SOS. I. Occurrence and Polymorphic Transformation, *J. Am. Oil Chem. Soc. 66*:664–674 (1989).
6. Chapman, D., The Polymorphism of Glycerides, *Chem. Rev. 62*:433–456 (1962).
7. Lutton, E.S., F.L. Jackson, and O.T. Quimby, The Polymorphism of the Mixed Triglycerides of Palmitic and Stearic Acids, *J. Am. Chem. Soc. 70*:2441–2445 (1948).
8. Gibon, V., F. Durant, and C. Deroanne, Polymorphism and Intersolubility of Some Palmitic, Stearic and Oleic Triglycerides: PPP, PSP and POP, *J. Am. Oil Chem. Soc. 63*:1047–1055 (1986).
9. Van Putte, K.P.A.M., and B.H. Bakker, Crystallization Kinetics of Palm Oil, *Ibid. 64*:1138–1143 (1987).
10. Timms, R.E., Crystallization of Fats, in *Developments in Fats and Oils*, edited by R.J. Hamilton, Blackie Academic, New York, 1995, pp. 204–223.
11. deMan, L., J.M. deMan, and B. Blackman, Effect of Tempering on the Texture and Polymorphic Behavior of Margarine Fats, *Fat Sci. Technol. 97*:55–60 (1995).
12. Gray, M.S., N.V. Lovegren, and R.O. Feuge, Effect of 2-Oleodipalmitin and 2-Elaidopalmitin on Polymorphic Behavior of Cocoa Butter, *J. Am. Oil Chem. Soc. 53*:727–731 (1976).
13. Rousseau, D., K. Forestière, A.R. Hill, and A.G. Marangoni, Restructuring Butter Fat Through Blending and Chemical Interesterification. 1. Melting Behavior and Triacylglycerol Modifications, *Ibid. 73*:963–972 (1996).
14. Norton, I.T., C.D. Lee-Tuffnell, S. Ablett, and S.M. Bociek, A Calorimetric, NMR and X-Ray Diffraction Study of the Melting Behavior of Tripalmitin and Tristearin and Their Mixing Behavior with Triolein, *Ibid. 62*:1237–1244 (1985).
15. Elisabettini, P., A. Desmedt, V. Gibon, and F. Durant, Effect of Sorbitan Tristearate on the Thermal and Structural Properties of Monoacid Triglycerides—Influence of a "Cis" or "Trans" Double Bond, *Fat. Sci. Technol. 97*:65–69 (1995).
16. Larsson, K., Hydrocarbon Chain Conformation in Fats, *Chemica Scr. 1*:21–23 (1971).
17. Hernqvist, L., On the Crystal Structure of the β1′-Form of Triglycerides and the Mechanism Behind the β1′→β Transition of Fats, *Fat Sci. Technol. 90*:451–454 (1988).
18. Lutton, E.S., Lipid Structures, *J. Am. Oil Chem. Soc. 49*:1–9 (1972).
19. Dafler, J.R., Polymorphism Behavior in Fully Hydrogenated Mono Acid Triglycerides, *Ibid. 54*:249–254 (1977).
20. Schlichter Aronhime, J., S. Sarig, and N. Garti, Dynamic Control of Polymorphic Transformation in Triglycerides by Surfactants: The Button Syndrome, *Ibid. 65*:1144–1150 (1988).

[Received March 4, 2004; accepted December 6, 2004]